A multilevel approach to cancer growth modeling

P.P. Delsanto[a,*,1], C.A. Condat[c], N. Pugno[b], A.S. Gliozzi[a], M. Griffa[d,1]

[a]Department of Physics, Politecnico di Torino, Corso Duca degli Abruzzi 24, 10129 Torino, Italy
[b]Department of Structural Engineering, Politecnico di Torino, Corso Duca degli Abruzzi 24, 10129 Torino, Italy
[c]CONICET and FaMAF, Universidad Nacional de Córdoba, 5000-Córdoba, Argentina
[d]EES-11, MS D443, Los Alamos National Laboratory, Los Alamos, NM, USA

Abstract

Cancer growth models may be divided into macroscopic models, which describe the tumor as a single entity, and microscopic ones, which consider the tumor as a complex system whose behavior emerges from the local dynamics of its basic components, the neoplastic cells. Mesoscopic models (e.g. as based on the Local Interaction Simulation Approach [Delsanto, P.P., Mignogna, R., Scalerandi, M., Schechter, R., 1998. In: Delsanto, P.P. Saenz, A.W. (Eds.), New Perspectives on Problems in Classical and Quantum Physics, vol. 2. Gordon & Breach, New Delhi, p. 5174]), which explicitly consider the behavior of cell clusters and their interactions, may be used instead of the microscopic ones, in order to study the properties of cancer biology that strongly depend on the interactions of small groups of cells at intermediate spatial and temporal scales. All these approaches have been developed independently, which limits their usefulness, since they all include relevant features and information that should be cross-correlated for a deeper understanding of the mechanisms involved.

In this contribution we consider multicellular tumor spheroids as biological reference systems and propose an intermediate model to bridge the gap between a macroscopic formulation of tumor growth and a mesoscopic one. Thus we are able to establish, as an important result of our formalism, a direct correspondence between parameters characterizing processes occurring at different scales. In particular, we analyze their dependence on an important limiting factor to tumor growth, i.e. the extra-cellular matrix pressure. Since the macro and meso-models stem from totally different roots (energy conservation and clinical observations vs. cell groups dynamics), their consistency may be used to validate both approaches. It may also be interesting to note that the proposed formalism fits well into a recently proposed conjecture of growth laws universality.

© 2007 Elsevier Ltd. All rights reserved.

PACS: 87.17.Aa; 05.65.+b; 87.18.Bb; 89.75.Da

Keywords: Cancer growth; Multicellular tumor spheroids; Modeling; Scaling; Multilevel approach; Cellular dynamics; Universality; Energy balance; Complexity

1. Introduction

Crucial to our understanding of the development of complexity is our ability to relate phenomena occurring at different scales. This is necessary not only to predict the emergence of macroscopic phenomena from microscopic processes, but also to relate microscopic variables to the more accessible parameters of macroscopic phenomenology. In fact, the use of more realistic values for the parameters of the microscopic (and mesoscopic) simulations may greatly enhance their predictive potentiality and, therefore, their applicability for biomedical and/or clinical purposes. As a rule, numerical simulations are necessary to implement microscopic or mesoscopic models, while analytical (or semi-analytical) solutions are usually possible for macroscopic models.

Tumors are remarkable examples of complex self-organizing systems. Due to their inherent complexity, it is

*Corresponding author: Tel.: +39 115647320; fax: +39 115647399.

E-mail addresses: pier.delsanto@polito.it (P.P. Delsanto), condat@famaf.unc.edu.ar (C.A. Condat), nicola.pugno@polito.it (N. Pugno), antonio.gliozzi@polito.it (A.S. Gliozzi), mgriffa@lanl.gov (M. Griffa).

[1]Also at: Bioinformatics and High Performance Computing Lab, Bioindustry Park of Canavese, Via Ribes 5, 10100, Colleretto Giacosa (TO), Italy.

necessary to analyze their growth at different scales. In a macroscopic approach, we consider them as single entities, whose behavior can be predicted in terms of their global interaction with the environment and a few internal parameters. This approach has led to a host of useful models of cellular population dynamics in different biological systems (for example cell cultures, Murray, 2004, the immune system, Adam and Bellomo, 1996; Perelson and Weisbuch, 1997, neoplastic masses, Adam and Bellomo, 1996; Preziosi, 2003).

Interest in this approach has been further rekindled by the conjecture of Guiot et al. (2003) that the ontogenetic growth law for all living organisms of West, Brown, and Enquist (WBE) (West et al., 1999, 2001) may be fruitfully extended to cancer growth. In the form proposed by WBE, this law states that two hypotheses suffice to ensure the existence of a universal growth dynamics: the conservation of energy and the presence of a fractal distribution network for energy supply at each part of the biological system considered. These basic hypotheses lead to the well-known exponent ($p = 3/4$) in the relationship between metabolic rate and mass scaling, which is purportedly characteristic of all organisms.

In a *microscopic* description, one should identify individual cell properties and predict tumor development from cell–cell interactions. Such an approach has two drawbacks: first, cancer growth is a collective phenomenon whose complexity may not emerge from the ensemble of its individual cell properties alone. Second, the huge number of cells involved (typically 10^8 cells for a $1\,cm^3$ tumor) restricts considerably the feasibility of simulations taking into account the behavior and dynamics of each individual cell, unless populations with a small number of individuals can be considered. As a consequence, *mesoscopic* models (Scalerandi et al., 1999, 2001; Sansone et al., 2001; Ferreira et al., 2002; Scalerandi et al., 2002; Scalerandi and Sansone, 2002; Chen et al., 2003) have been proposed, in which the coarse graining of the system, and the behavior of cell clusters and their interactions is considered. Mesoscopic models are also better adapted to describe the influence of the macroscale world on microscale phenomena and vice versa. A nice exposition of the insights that mathematical modeling can yield about the mechanisms underpinning the great complexity of the various phases of cancer growth is presented in a recent review by Byrne et al. (2006). Among other recent papers about modeling tumor growth, we can quote another review paper by Alarcón et al. (2005) or, more generally, refer to the repository of mathematical models and corresponding computational codes assembled within the framework of the CViT (Center for the development of a Virtual Tumor) Project (http://www.cvit.org), belonging to the US NIH-NCI ICBP (Integrative Cancer Biology Program).

Multicellular Tumor Spheroids (MTSs) represent convenient experimental systems for analyzing and comparing tumor growth models at different levels. They are spherical aggregations of tumor cells that may be grown *in vitro* under strictly controlled conditions, mimicking some of the important features of solid tumors developing *in vivo* (Hamilton, 1998; Thomson and Byrne, 1999; Mueller-Klieser, 2000; Chignola et al., 2000; Kelm et al., 2003). Due to their simple geometry, the possibility of culturing them in large quantities and of controlling relevant parameters, such as the porosity and stiffness of the surrounding environment, they are excellent systems upon which to test the applicability of various models (Marusic et al., 1994; Delsanto et al., 2004, 2005a). Experimental spheroid setups are designed to provide a suitable amount of oxygen and other nutrients, which diffuse to the outer edges of the MTS, and then to the interior. Due to consumption by the outer region, nutrient concentration decreases towards the center. Consequently, as it has been observed, proliferating cells are usually present in the outermost shell, quiescent (nonreproductive) cells dominate in the interior, and, eventually at a later stage of growth, a necrotic core is formed by dead cells. An MTS is thus a heterogeneous cellular system of considerable complexity, but whose properties and growth can be carefully monitored and modeled.

Using MTS's as working models (but with the expectation that our conclusions may be applied also to the study of some aspects of *in vivo* tumor growth), we review in Sections 2 and 3, two recently proposed growth models at the mesoscopic (Delsanto et al., 2005b) and macroscopic (Guiot et al., 2003; Delsanto et al., 2004) levels, respectively. The latter is extended in order to take into account the pressure exerted by the growing tumor against its environment. This term plays a crucial role in the mechanisms involved in tumoral invasion (Guiot et al., 2006b), which ultimately represents the procedure which allows further growth of tumors *in vivo*. Then, in Section 4, we show that it is possible to formulate a coherent picture embodying both descriptions by means of an Intermediate Model (IM) (Delsanto et al., 2005a). A detailed description of the IM and of the relationship (mediated by the IM) between the mesoscopic and macroscopic parameters represents the main goal of the present contribution.

2. A link to cell dynamics: mesoscopic model

In this Section we review the mesoscopic MTS model of Delsanto et al. (2005b). In this model space is divided into concentric isovolumetric shells $n = 0, \ldots, N$ ($n = 0$ labels the central sphere of radius r_0). Each shell has a volume $V_0 = (\frac{4}{3})\pi r_0^3$, and a correspondence is established between the shell system and a one-dimensional grid. The center of the shell system coincides with the location of the implanted spheroid seed. The MTS growth is controlled by local nutrient availability and proceeds according to the following rules (see Fig. 1):

(a) Feeding: nutrient is absorbed by each shell at a rate γc_n, where c_n is the number of live cancer cells in the *n*th shell.
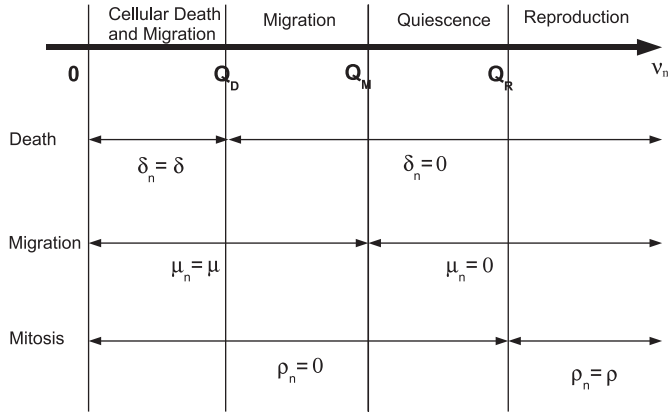
Fig. 1. Schematic representation of the basic cellular processes in the nth MTS shell as a function of the number of available nutrient units v_n. The three lines below the v_n axis imply that cellular death occurs only for $v_n < Q_D$, migration for $v_n < Q_M$ and cell reproduction for $v_n > Q_R$, respectively. Correspondingly, the three parameters δ_n, μ_n and ρ_n are different from zero (and equal to δ, μ and ρ) only for $v_n < Q_M$, $v_n < Q_M$ and $v_n > Q_R$, respectively.

(b) Reproduction: cancer cells reproduce, at rates $\rho_n c_n$, only in the shells where the number v_n of locally available nutrient units exceeds a given threshold Q_R.

(c) Migration: cells migrate to adjacent shells with a flux $\mu_n c_n$ per unit of grid cell surface if the number of nutrient units falls below a threshold Q_M. Since nutrients diffuse inwards, migration will usually proceed towards outer shells. We may plausibly assume that outwards migration is also favored by mechanical stress gradients (Gordon et al., 2003). Due to the bias introduced by the radial gradients, we distinguish between outwards (μ^+) and inwards (μ^-) migration fluxes.

(d) Death: cell death occurs (at rates $\delta_n c_n$) where the number of nutrient units falls below the threshold Q_D.

The thresholds satisfy the conditions $Q_D < Q_M < Q_R$. Fig. 1 summarizes in a simple scheme the set of thresholds associated to the different biological/biophysical phenomena and the corresponding value ranges for the rates. As reported in Griffa et al. (2004) the actual implementation of the model makes use of sigmoidal functions for representing the rates dependence on nutrient concentration instead of Heaviside functions (i.e. thresholds).

Nutrients diffuse from the nth shell to the adjacent ones at a rate αv_n per unit area. Since cellular displacement and molecular diffusion between shells are proportional to the areas of the separating surfaces, the diffusion terms across the interface between the $(n-1)$th and nth shells will be proportional to $n^{2/3}$. The model equations are then written directly in their time-discretized forms:

$$c_n^* = c_n(1 - \tau\delta_n + \tau\rho_n) + \tau r_0^2[n^{2/3}(\mu_{n-1}^+ c_{n-1} - \mu_n^- c_n) + (n+1)^{2/3}(\mu_{n+1}^- c_{n+1} - \mu_n^+ c_n)], \tag{1}$$

$$d_n^* = d_n + \tau\delta_n c_n - \tau\lambda_n d_n, \tag{2}$$

$$v_n^* = v_n - \tau\gamma c_n + \tau\alpha r_0^2[n^{2/3}(v_{n-1} - v_n) + (n+1)^{2/3}(v_{n+1} - v_n)], \tag{3}$$

where τ is the time step and the asterisk means that the corresponding quantity must be evaluated at the time $t + \tau$, instead of at the time t. In Eq. (2) d_n is the number of dead cells in the nth shell; the last term, with a coefficient λ_n, has been added to account for possible disintegration of dead cells releasing intracellular fluid (Cristini et al., 2005; Frieboes et al., 2006).

Numerical simulations based on the above model show that, in agreement with experimental observations, in a first stage the spheroid is fully populated by proliferating cells. Then, in the inside, cells become quiescent, i.e. alive but not proliferating, with a "wavefront" of proliferating cells which have greater probability of undergoing an outward migration due to the second type of movement mechanism implemented in the model, the one based on a smoothed cell density-per each shell threshold, as explained in Griffa et al. (2004). This *in silico* mechanism corresponds to the biomechanical stress-mediated transport of cells towards regions with lower levels of cell density, packing and deformation, due to both passive (purely elastic) and cell-mediated responses (Vernon et al., 1992; Dembo and Wang, 1999; Gordon et al., 2003; Deisboeck et al., 2005) to mechanical deformations. Finally, at later times, a predominantly necrotic core develops. According to the model implementation, when the total number of living-plus-dead cells in the nth shell is larger than a given threshold, the probability per unit of time of migration towards the nearest neighbor shells arises, so that some cells leave that shell. The threshold value is a function of the cell mean radius and of r_0. Thus, the mechanical stress-driven migration is essentially triggered by the unbalance between the volume of each shell and the one occupied by the living and dead cells. If the latter is too large, a higher level of packing and cell deformation occurs with mass transport as consequence. Different weights are assigned in computing the volume occupied by the living vs. dead cells, in order to account for their different deformation. Also, a rigid Heaviside function is replaced by a sigmoid (see Griffa et al. (2004) for the mathematical detail). Fig. 2 shows the radial distribution of viable cells within the simulated spheroid at three different time steps belonging respectively to the three cited stages of growth. The simulation aims at reproducing the typical layout of an MTS in terms of cell state spatial distribution.

3. A link to phenomenology: macroscopic model

Both the discussion in the Introduction and Fig. 2 suggest the use of a three-layer macroscopic model for the tumor. Using the WBE model, as extended to tumors by Guiot et al. (2003), we assume that a central core of dead cells (region Z_0) is surrounded by a first layer Z_1 of quiescent cells, and by an outer layer Z_2 of active cells and
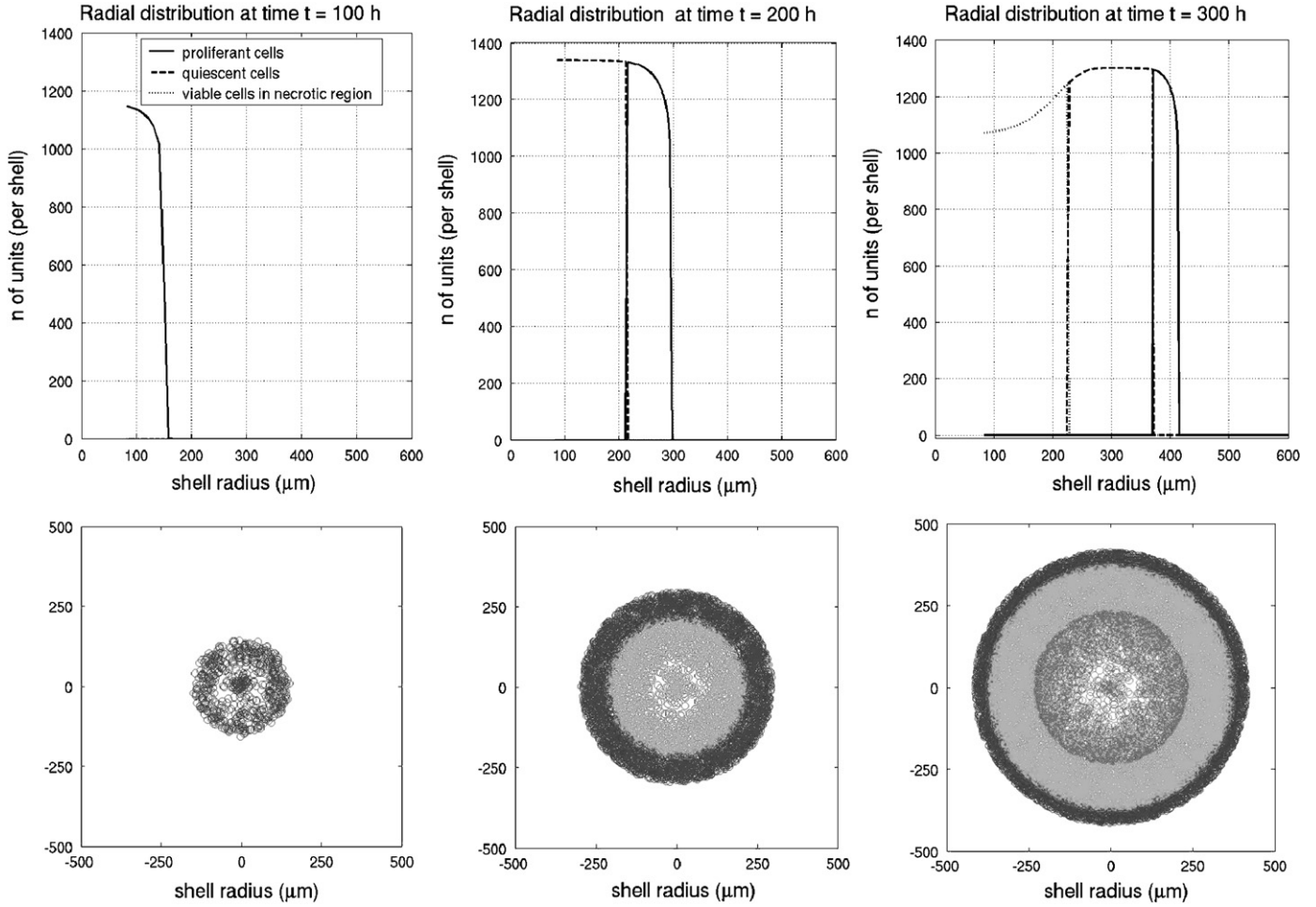
Fig. 2. The three stages of development of a MTS, as obtained from a mesoscopic simulation at three successive times. In the first stage all cells are proliferating. In the second one a region of quiescent cells emerges and soon occupies most of the interior. In the third one a necrotic core develops, which, however, includes some viable cells in the process of dying (especially at its rim). The mesoscopic parameters for the simulations are $\mu = 0.003$, $\rho = 0.025$, $\delta = 0.01$, $\sigma = 1.7$ in the nonzero zones defined in Fig. 1.

neglect, as temporary, any mixing, i.e. the presence of cells in the "wrong" regions. We label the three cell species 0, 1, and 2 respectively, and call their corresponding masses m_i ($i = 0, 1, 2$). It is important to remark that the central core Z_0 and the two layers Z_1 and Z_2 need not to be spherical, i.e. the macroscopic model may be used to describe not only MTS's, but also almost any kind of pre-vascular *in vivo* solid cancers.

Since energy is transported to the tumor cells by the diffusing nutrients, we assume that it is proportional to the amount of the latter. Therefore, applying the law of energy conservation as in Delsanto et al. (2004), we may write the energy balance for region Z_2 as,

$$B_2 \, \mathrm{d}t = N_2 \xi_2 \, \mathrm{d}t + \varepsilon \, \mathrm{d}N_2 + \chi \, \mathrm{d}N_2, \qquad (4)$$

where

$$\chi = \left(\frac{\kappa P M}{\zeta} \right) \qquad (5)$$

and N_2 is the total number of cancer cells in Z_2 at time t, P is the hydrostatic pressure on the spheroid wall, B_2 is the

net nutrient-associated energy inflow into Z_2 during the interval $\mathrm{d}t$, ζ is the mass density, assumed to be uniform, ξ_2 is the metabolic rate for a single cancer cell, and ε is the energy required to create a new cell in a "soft" environment. If M is the mass of a single cell, $m_2 = M N_2$.

In Eq. (4) the last term on the right-hand-side is new with respect to Delsanto et al. (2004), and represents the amount of energy required by the volumetric expansion. It includes not only the mechanical work done by the biologically growing system against its environment at pressure P, i.e. (from thermodynamics) $P \, \mathrm{d}V_2$, which is comparatively small (and would correspond to a value of $\kappa = 1$), but also the excess energy required to create new biological material in a stressed environment. Such excess energy is the result of complex biological processes and can be assumed (at least as a first approximation) to be proportional to the volume increase, $\mathrm{d}V_2 = M \, \mathrm{d}N_2$.

Two plausible and complementary assumptions can be formulated regarding the pressure dependence, as a function of the constitutive laws of the matrix and tumor materials. In a recent paper Guiot et al. (2006b),

the interface pressure increases due to the tumor elastic growth, until a characteristic strength of the matrix is reached, the stress released and a new annular region of matrix colonized by the tumor. In this model a perfectly plastic constitutive law for the matrix is also assumed, corresponding to a strain flow at a given value P. For such a case the pressure P is expected to be constant, representing the yielding strength of the matrix material. Obviously these two assumptions represent limit conditions of a more complex reality, but the introduction of P represents an important novelty with respect to previous models (for which $P = 0$), due to the role of mechanical stress in triggering and controlling various biomechanical and biophysical processes (Chaplain et al., 2006), both at the single cell level (remodulation of intracellular structures by the cell deformation and consequent change in gene expression and protein synthesis, Ingber et al., 1995) and at the multicellular one (change of intercellular communications via release of molecules, apoptosis and cell proliferation control via the change of cell adhesion, Shraiman, 2005; Hufnagel et al., 2007; Helmlinger et al., 1997).

The left-hand side of Eq. (4), $B_2\,dt$, describes the energy necessary for the overall thermodynamic processes occurring within the cell population occupying the region Z_2. This energy, as previously stated, results from the balance of two different flows of nutrients molecules (the carriers of energy for every metabolic process): the total diffusive inflow towards the spheroid, which is proportional to a power p_2 of its whole mass, according to the general law relating the mass of a biological system and the rate of energy inflow needed for maintenance and proliferation (West et al., 1999, 2001; Guiot et al., 2003), and the nutrient molecules flow towards the inner region Z_1, which produces an energy leakage rate for the Z_2 population, but an energy acquisition rate for the Z_1 one proportional to the p_1 power of its mass, according to the same law. Thus,

$$B_2 = B_{02}(m_0 + m_1 + m_2)^{p_2} - B_{01}(m_0 + m_1)^{p_1}, \qquad (6)$$

where B_{01} and B_{02} are constants. The assumption that cellular feeding is controlled only by diffusive processes, i.e. that the tumor is in a pre-vascular stage, would imply that $p_1 = p_2 = \frac{2}{3}$, because the inflow through the surface is proportional to the $\frac{2}{3}$ power of the volume. By contrast WBE's law assumes that resources are transported to the cells through a fractal hierarchical branching network (West et al., 1999), which implies $p = \frac{3}{4}$. In fact, the power law dependence of B on m has been recognized for a long time (Kleiber, 1932), but the value of the exponent and its ultimate meaning are still sources of controversy (Dodds et al., 2001; Makarieva et al., 2003). It has been recently pointed out that our model (and in particular a careful monitoring of the p exponent) may enable us to predict the progression of a tumor (Guiot et al., 2006a; Carpinteri and Pugno, 2005; Guiot et al., 2006b).

On heuristically justified grounds, we can also apply the same formulation to describe cell evolution in Z_0 and Z_1, using the same approach and the same type of rules which connect the energy rate consumed by a cell population to its total mass through a power law. By extending the definition of B_{02} and ξ_2 to the other two regions and using Eqs. (4) and (6), the subsequent equation for the temporal evolution of the masses of each cell population is obtained:

$$\frac{dm_i}{dt} = a_i \left(\sum_{j=0}^{i} m_j \right)^{p_i} - a_{i-1} \left(\sum_{j=0}^{i-1} m_j \right)^{p_{i-1}} - b_i m_i, \qquad (7)$$

where m_i is the total mass of the ith population, for $i = 0, 1, 2$, and

$$a_i = \frac{MB_{0i}}{\varepsilon + \kappa PM/\zeta}, \qquad (8)$$

$$b_i = \frac{\xi_i}{\varepsilon + \kappa PM/\zeta}, \qquad (9)$$

with $a_{-1} = 0$. The growth of the tumor mass in each region is proportional to the difference between the net energy input (first term minus second term) in Eq. (7) and the amount of energy used for cell maintenance (third term). Eqs. (7)–(9) define a consistent phenomenological model whose parameters may be evaluated from the results of macroscopic experiments. They belong to a class, called U2, of a recently proposed classification scheme for phenomenological universalities in growth problems (Castorina et al., 2006). U2 includes, as special cases, the WBE, the logistic and all the other previously proposed growth models. The introduction of the expansion term in Eq. (4) leads to a reduction in the size of most of the coefficients, a fact whose consequences will be explored later. The outer shell coefficients a_2 and b_2 can be obtained from experimental observations of the whole spheroid (Condat and Menchón, 2006). The coefficients a_0 and b_0 can be obtained form observations of the necrotic core.

If we assume that necrotic cells do not consume energy $\xi_0 = 0$. Then $b_0 = 0$ and Eq. (7) for m_0 can be straightforwardly solved, yielding,

$$m_0(t) = [(\tilde{m})^{1-p_0} + a_0(1-p_0)(t-t_0)]^{1/(1-p_0)}, \qquad (10)$$

where $p_0 \neq 1$ and $\tilde{m}$ is the mass at time t_0. If we choose t_0 as the time of onset of the necrotic core, $\tilde{m} = 0$. At long times the necrotic mass increases as a power law; in particular, if $p_0 = \frac{2}{3}$, $m_0(t) \sim t^3$. For $p_0 = 1$, there is exponential growth at all times. Since a_0 is expected to decrease with increasing pressure, the necrotic core (and the rest of the tumor) will grow more slowly under conditions of higher pressure. A tumor steady state can be obtained from Eqs. (7) only if $b_0 \neq 0$.

4. The bridge: intermediate model

To formulate an auxiliary model that allows us to bridge the gap between the mesoscopic and macroscopic descriptions, we start by rewriting the equation describing the evolution of the number of cancer cells in the nth

mesoscopic shell as a first order differential equation that explicitly exhibits the cell fluxes. Assuming that the time step τ is very small, we write,

$$c_n^* - c_n \approx \tau \frac{\mathrm{d}c_n}{\mathrm{d}t}. \tag{11}$$

The mesoscopic equation (1) then becomes

$$\frac{\mathrm{d}c_n}{\mathrm{d}t} = \beta_n c_n + \Phi_{n-1} - \Psi_{n-1} + \Psi_n - \Phi_n, \tag{12}$$

where Φ_n and Ψ_n stand for the outward and inward cell flows, respectively,

$$\Phi_n = (n+1)^{2/3} r_0^2 \mu_n^+ c_n, \tag{13}$$

$$\Psi_n = (n+1)^{2/3} r_0^2 \mu_{n+1}^- c_{n+1}, \tag{14}$$

where $\beta_n = \rho_n - \delta_n$ is the difference between the reproduction and death rates, except in Z_0 where $\beta_n = -\lambda_n$.

Next we regroup the shells with $n \leqslant n_0$, $n_0 < n \leqslant n_1$ and $n_1 < n \leqslant n_2 = N$ in the three regions, Z_0, Z_1 and Z_2, respectively. Although the equation describing the nutrient evolution in the mesoscopic model (Eq. (3)) is not explicitly considered, the role of the nutrient distribution is clear: since the nutrient comes from outside and is progressively consumed (or stored for later consumption) by the viable cells inside, the above stratification is a reasonable approximation (Mueller-Klieser, 2000). Of course, due to the randomness inherent to the involved processes, we would expect a smoother distribution in the experimental data. In order to set the model in a form adequate for the comparison, we proceed as follows:

1. At each discretization step we will conceptually separate the description of growth into two stages. In the first stage cells multiply, migrate and die, but the volumes of the various zones are kept constant. In the second stage, the zone radii are allowed to vary in order to restore cell concentration uniformity. Therefore the rescaled zone volumes "recapture" the cells that left each zone during the first step; this corresponds to a loss of mass $-\mathrm{d}m_i$ for the zone Z_i.
2. Since we are solely interested in the number of cells inside each region, we can sum over the contributions of all its shells. Internal migrations in each region do not affect the number of cells therein and are therefore irrelevant. The only migration terms that matter are those across the region boundaries, that is to the shells $n = n_0$, n_1 and $n_2 = N$.
3. By definition, all cells are included in the MTS; thus, no cells can enter from the outside: $\Psi_{n_2} = 0$. We will disregard the centripetal migrations Ψ_{n_0} and Ψ_{n_1} since they would amount to including active cells in Z_1 or quiescent ones in Z_0 (which is forbidden by our definition of the regions). Operationally, this implies setting the transport coefficients $\mu_{n_i}^- = 0$ at the region edges. Alternatively, we may redefine $\bar{\Phi}_n$ as the net balance $\Phi_n - \Psi_n$.

4. As a coarse grain approximation, the rates δ_n, ρ_n and λ_n may be reasonably equated in each region to their asymptotic values or to 0 as a consequence of the sigmoidal functions implementing their dependence from nutrient concentrations. This corresponds to selecting very steep sigmoidal functions (Griffa et al., 2004). It follows that $\delta_n = \rho_n = 0$ in the first (necrotic) region, since dead cells cannot die or reproduce; we also fix $\lambda_n = \lambda$ in the same region. In Z_1 we set $\delta_n = \delta$ and $\rho_n = 0$, while in Z_2 we write $\delta_n = 0$ and $\rho_n = \rho$, with both ρ and δ being the asymptotic values of the corresponding variables.

With the above assumptions, we can use the set of equations (12) to obtain equations for the total numbers of cells $\bar{c}_i = \sum c_j$ in their respective regions Z_i ($i = 0, 1, 2$). Summing Eqs. (12) over n for all the shells included in each of the three regions Z_i, we obtain

$$\frac{\mathrm{d}\bar{c}_2}{\mathrm{d}t} = \rho \bar{c}_2 + \bar{\Phi}_{n_1} - \bar{\Phi}_{n_2}, \tag{15}$$

$$\frac{\mathrm{d}\bar{c}_1}{\mathrm{d}t} = -\delta \bar{c}_1 + \bar{\Phi}_{n_0} - \bar{\Phi}_{n_1}, \tag{16}$$

$$\frac{\mathrm{d}\bar{c}_0}{\mathrm{d}t} = -\bar{\Phi}_{n_0} - \lambda \bar{c}_0. \tag{17}$$

The outward cell flux from the outermost shell of each region Z_i ($i = 0, 1, 2$) across the surface separating it from the next region (the matrix in the case $i = 2$) can be renamed as $\bar{\Phi}_i$: $\bar{\Phi}_0 = \bar{\Phi}_{n_0}$, $\bar{\Phi}_1 = \bar{\Phi}_{n_1}$ and $\bar{\Phi}_2 = \bar{\Phi}_{n_2}$, where $n_2 = N$.

In Eq. (16) $\delta \bar{c}_1$ is the total dying cell rate. Since cells in the necrotic core may only be reabsorbed, the only contributions to cell variation in Z_0 are given by the flux $-\bar{\Phi}_0$ and the absorption $-\lambda \bar{c}_0$.

Next we evaluate the fluxes $\bar{\Phi}_i$. The factor $r_0^2(n+1)^{2/3}$ in Eqs. (13) and (14), for $n = n_i$ ($i = 0, 1, 2$), corresponds to the square of the external radius, R_i^2, of the corresponding zone, Z_i. Because migrations to other regions start only from the outermost shell in each region, the fluxes will be proportional to $\eta \mu_i$ ($i = 0, 1, 2$), where $\mu_i \equiv \mu_{n_i}^+$ is the local mobility and $\eta = c_{n_i}$ is the mean number of cells in the n_ith isovolumetric shell. We keep η approximately constant because of the migration mechanism based on the mechanical stress-driven mass transport. In fact the outer shell of each zone is subject to an outwards chemotaxis-based cell migration due to the gradient in the concentration of nutrients (Dorie et al., 1982, 1986; McElwain and Pettet, 1993) (which tends to increase local cell density), but also to the mechanical opposition of the external cells (or the extracellular matrix in the case of the proliferant rim Z_2). The intermediate increase of cell density is then compensated by the stress-driven migration (invasion in the case of the proliferative rim), in order not to increase the cell density above its maximum allowed value (Deisboeck et al., 2005). The constant cell density assumption in the formulation of

the IM is in agreement with many experimental observations (Freyer and Sutherland, 1986b, 1985, 1980), although other recent investigations (Nirmala et al., 2001) show that it may slightly vary in time and space due to the local heterogeneities at smaller scales within the MTS. The fluxes can be written as

$$\bar{\Phi}_i = \mu_i c_{n_i} R_i^2 = \mu_i \eta \left(\frac{3}{4\pi\zeta} \sum_{j=0}^{i} m_j \right)^{2/3}. \tag{18}$$

Next, we correlate Eq. (7) for the mass variations with Eqs. (15)–(17) for the variations in cell numbers. Using the two-stages model at each discretization step, as discussed before, from $m_i = M\bar{c}_i$, it follows

$$\frac{\mathrm{d}\bar{c}_i}{\mathrm{d}t} = -\frac{1}{M} \frac{\mathrm{d}m_i}{\mathrm{d}t}. \tag{19}$$

Now we can combine Eqs. (15)–(19) to write the equations for the mass variations in each of the three zones:

$$\frac{\mathrm{d}m_2}{\mathrm{d}t} = -\rho m_2 - \sigma\mu_1(m_0 + m_1)^{2/3} + \sigma\mu_2(m_0 + m_1 + m_2)^{2/3}, \tag{20}$$

$$\frac{\mathrm{d}m_1}{\mathrm{d}t} = -\delta m_1 - \sigma\mu_0 m_0^{2/3} + \sigma\mu_1(m_0 + m_1)^{2/3}, \tag{21}$$

and

$$\frac{\mathrm{d}m_0}{\mathrm{d}t} = -\lambda m_0 + \sigma\mu_0 m_0^{2/3}, \tag{22}$$

where

$$\sigma = M\eta \left(\frac{4\pi}{3}\zeta \right)^{-2/3}. \tag{23}$$

By comparing Eq. (7) with Eqs. (20)–(22), we find that both models coincide if the following parameter identification is performed.

$$a_0 = \sigma\mu_0, \quad a_1 = \sigma\mu_1, \quad a_2 = \sigma\mu_2, \tag{24}$$

$$b_0 = -\lambda, \quad b_1 = -\delta, \quad b_2 = \rho \tag{25}$$

and

$$p_0 = p_1 = p_2 = \tfrac{2}{3}. \tag{26}$$

We have thus related the parameters corresponding to the mesoscopic and macroscopic formulations. That $p_i = \tfrac{2}{3}$ was to be expected by the construction of the mesoscopic model, but the other relations provide us with information about the dependence of the mesoscopic parameters on pressure. For instance, the interzone migration fluxes must decrease with increasing pressure,

$$\mu_i = \frac{MB_{0i}}{\sigma\left(\varepsilon + \frac{\kappa PM}{\zeta}\right)}. \tag{27}$$

This is reasonable, because migration is hindered by the increased cell concentration. The reproduction rate is decreased by the same factor:

$$\rho = \frac{\xi_2}{\varepsilon + \frac{\kappa PM}{\zeta}}, \tag{28}$$

which is also consistent with predictions put forward on the basis of experimental data (Helmlinger et al., 1997). Since it is not a priori clear what the dependence of b_0 and b_1 on P should be, we cannot draw general conclusions on the mesoscopic coefficients λ and δ. However, if we assume that the dependence of b_1 on P is the same as that of b_2, then we can conclude that the death rate is decreased by increasing pressure, a somewhat surprising result, which however, agrees with the results of Helmlinger et al. (1997), who observed that solid mechanical stress decreases the apoptotic rate. This decrease in the apoptotic rate is likely to be due to increased packing and concomitantly enhanced cell–cell interactions, which trigger the suppression of apoptotic cell death. Moreover, $\delta > 0$ implies $b_1 < 0$, that is, the proliferating-to-quiescent bulk transformation is faster than the quiescent-to-dead bulk transformation. Similarly, $\lambda > 0$ implies that the bulk dying rate must be larger than the reabsorption rate.

5. Conclusions

Through the introduction of an intermediate model, we have proved the consistency of two very different models for heterogeneous MTS growth: a macroscopic model, based on the ontogenetic growth model of West, Brown and Enquist, and a mesoscopic one, based on the coarse-graining of the cell system. Besides its intrinsic importance as a bridging tool, this unification helps us to establish a correspondence between hard-to-measure microscopic parameters and their more accessible macroscopic counterparts (see e.g. Fig. 3). The correspondence between the two models is remarkable, since they stem from completely different approaches, as stated in the Introduction. It is important to note that:

1. The IM model in its present form is not self-standing, i.e. it cannot by itself be used for actual simulations, since it implicitly depends on the evolving nutrient distribution (provided by the Eq. (3) in the mesoscopic model).
2. The consumption rate of nutrients due to the metabolism, which is explicit in the mesoscopic model is only implicit in the IM, via the "ignored" Eq. (3). Thus the metabolism parameters b_i correspond to the "cell activity" parameters in β_i in the IM.
3. According to Eqs. (20) to (22), the parameters p_i are all equal to $\tfrac{2}{3}$, which indicates that feeding must be diffusion-controlled to ensure consistency between the models. However, the values of the parameters p_i depend on the nature of nutrient transport. For instance, MTS internal vascularization is likely to change their values. The present treatment lends itself
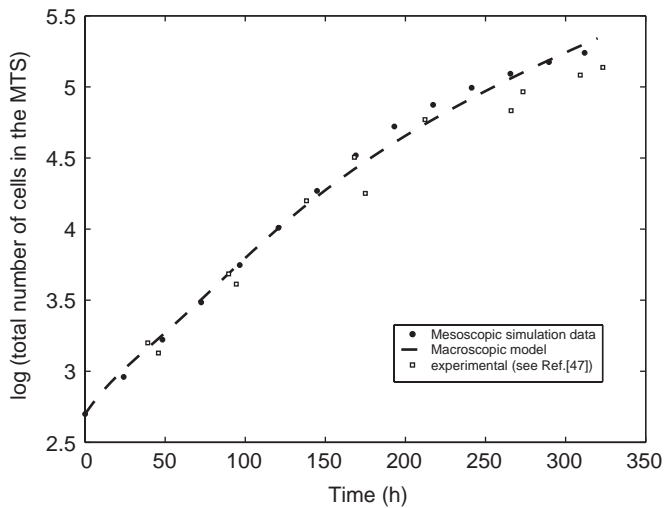
Fig. 3. Comparison between the results of a macroscopic (dashed line) and a mesoscopic (full dots) simulation with the experimental data (empty squares, Freyer and Sutherland, 1986a) referring to a MTS made of EMT6/Ro mouse mammary carcinoma cells grown in a culture medium. The parameters for the macroscopic simulations are: $a_1 = 0.15$, $a_2 = 0.48$, $a_3 = 0.59$, $b_0 = -0.012$, $b_1 = 0.0016$, $b_2 = 0.037$; the mesoscopic parameters are the same as in Fig. 2.

to suggest, through simulations and mathematical analysis, the relevance of the effects of different tumor microenvironments, some of which are easier to study *in vitro* or by implanting MTS in model laboratory animals (Oudar, 2000). For example, we could extend it to the case of underfeeding (Delsanto et al., 2004; Griffa and Scalerandi, 2005) and to the development of angiogenesis. In the latter case, it would be useful to find a connection between the various extant mesoscopic model (Dodds et al., 2001; Byrne and Chaplain, 1995; Byrne et al., 2006), and the simple predictions about the dependence of the growth rate on the instantaneous mass furnished by the macroscopic approach (Menchón and Condat, 2007). One could also explicitly consider the presence of growth inhibitors or consider the role of the necrotic mass in regulating the number of viable quiescent cells at the interface between the Z_0 and Z_1 regions. It is well known that necrotic death is closely related to the release of cytotoxic intra-cellular substances in the extra-cellular microenvironment (Greenspan, 1974; Freyer, 1988; Groebe and Mueller-Klieser, 1996). This process deserves to be considered with care. To conclude, we have used the simplest possible form for the dependence of the extra term in the WBE equation on the pressure. Our results could be easily generalized to more complicated cases by replacing κP in Eq. (4) with a suitable positive, monotonically increasing function $F(P)$. This would not introduce any qualitative changes in the results obtained here. Finally, we must remark that in our model the growth process is controlled by nutrient consumption and the possible influence of growth promoters/inhibitors is neglected. We also have neglected part of the cell–cell interactions and cell-cycle details (Jiang et al., 2005).

References

Adam, J.A., Bellomo, N. (Eds.), 1996. A Survey of Models for Tumor-Immune System Dynamics. Birkhauser, Basel.

Alarcón, T., Byrne, H.M., Maini, P.K., 2005. A multiple scale model for tumor growth. SIAM Multiscale Model. Simul. 3, 440.

Byrne, H.M., Chaplain, M.A.J., 1995. Mathematical models for tumour angiogenesis: numerical simulations and nonlinear wave solutions. Bull. Math. Biol. 57, 461.

Byrne, H.M., Alarcon, T., Owen, M.R., Webb, S.D., Maini, P.K., 2006. Modelling aspects of cancer dynamics: a review. Phil. Trans. Roy. Soc. A 364, 1563.

Carpinteri, A., Pugno, N., 2005. Are the scaling laws on strength of solids related to mechanics or to geometry? Nature Mat. 4, 421.

Castorina, P., Delsanto, P.P., Guiot, C., 2006. Classification scheme for phenomenological universalities in growth problems in physics and other sciences. Phys. Rev. Lett. 96, 188701.

Chaplain, M.A.J., Graziano, L., Preziosi, L., 2006. Mathematical modelling of the loss of tissue compression responsiveness and its role in solid tumour development. Math. Med. Biol. 23, 197–229.

Chen, W.Y., Annamreddy, P.R., Fan, L.T., 2003. Modeling growth of heterogeneous tumor. J. Theor. Biol. 221, 205.

Chignola, R., Schenetti, A., Chiesa, E., Foroni, R., Sartoris, S., Brendolan, A., Tridente, G., Andrighetto, G., Liberati, L., 2000. Forecasting the growth of multicell tumour spheroids: implication for the dynamic growth of solid tumours. Cell Prolif. 33, 219.

Condat, C.A., Menchón, S.A., 2006. Ontogenetic growth of multicellular tumor spheroids. Physica A 371, 76.

Cristini, V., Frieboes, H.B., Gatenby, R., Caserta, S., Ferrari, M., Sinek, J., 2005. Morphological instability and cancer invasion. Clin. Cancer Res. 11, 6772.

Deisboeck, T.S., Mansury, Y., Guiot, C., Degiorgis, P.G., Delsanto, P.P., 2005. Insights from a novel tumor model: indications for a quantitative link between tumor growth and invasion. Med. Hypotheses 65, 785.

Delsanto, P.P., Mignogna, R., Scalerandi, M., Schechter, R., 1998. In: Delsanto, P.P., Saenz, A.W. (Eds.), New Perspectives on Problems in Classical and Quantum Physics, vol. 2. Gordon & Breach, New Delhi, p. 5174.

Delsanto, P.P., Guiot, C., Degiorgis, P.G., Condat, C.A., Mansury, Y., Deisboeck, T., 2004. Growth model for multicellular tumor spheroids. Appl. Phys. Lett. 85, 4225.

Delsanto, P.P., Griffa, M., Condat, C.A., Delsanto, S., Morra, L., 2005a. Bridging the gap between mesoscopic and macroscopic models: the case of multicellular tumor spheroids. Phys. Rev. Lett. 94, 148105.

Delsanto, P.P., Morra, L., Delsanto, S., Griffa, M., Guiot, C., 2005b. Towards a Model of Local and Collective Mechanisms in Multicellular Tumor Spheroids Growth. Physica Scripta T118, 157.

Dembo, M., Wang, Y.L., 1999. Stresses at the cell-to-substrate interface during locomotion of fibroblasts. Biophys. J. 76, 2307.

Dodds, S., Rothman, D.H., Weitz, J.S., 2001. Re-examination of the 3/4-law of metabolism. J. Theor. Biol. 209, 9.

Dorie, M.J., Kallman, R.F., Rapacchietta, D.F., Van Antwerp, D., Rong Huang, Y., 1982. Migration and internalization of cells and polystyrene microspheres in tumour cell spheroids. Exp. Cell Res. 141, 201.

Dorie, M.J., Kallman, R.F., Coyne, M.A., 1986. Effect of cytochalasin B, nocodazole and irradiation on migration and internalization of cells and microspheres in tumor cell spheroids. Exp. Cell Res. 166, 370.

Ferreira, S.C., Martins, M.L., Vilela, M.J., 2002. Reaction-diffusion model for the growth of avascular tumor. Phys. Rev. E 65, 021907.

Freyer, J.P., 1988. Role of necrosis in regulating the growth saturation of multicellular spheroids. Cancer Res. 48, 2432.

Freyer, J.P., Sutherland, R.M., 1980. Selective dissociation and characterization of cells from different regions of multicell tumor spheroids. Cancer Res. 40, 3956.

Freyer, J.P., Sutherland, R.M., 1985. A reduction in the in situ rates of oxygen and glucose consumption of cells in EMT6/Ro spheroids during growth. J. Cell Phys. 124, 516.

Freyer, J.P., Sutherland, R.M., 1986a. Regulation of growth saturation and development of necrosis in EMT6/Ro multicellular spheroids by the glucose and oxygen supply. Cancer Res. 46, 3504.

Freyer, J.P., Sutherland, R.M., 1986b. Proliferative and clonogenic heterogeneity of cells from EMT6/Ro multicellular spheroids induced by the glucose and oxygen supply. Cancer Res. 46, 3513.

Frieboes, H.B., Zheng, X., Sun, Ch.-H., Tromberg, B., Gatenby, R., Cristini, V., 2006. An integrated computational/experimental model of tumor invasion. Cancer Res. 66, 1597.

Gordon, V.D., Valentine, M.T., Gardel, M.L., Andor, D., Dennison, S., Bogdanov, A.A., Weitz, D.A., Deisboeck, T.S., 2003. Measuring the mechanical stress induced by an expanding multicellular tumor system: a case study. Exp. Cell Res. 289, 58.

Greenspan, H.P., 1974. On the self-inhibited growth of cell cultures. Growth 38, 81.

Griffa, M., Scalerandi, M., 2005. Physical modeling and simulations of tumor growth and angiogenesis: predictions and new hypotheses. Physica Scripta T118, 183.

Griffa, M., Delsanto, S., Morra, L., Delsanto, P.P., 2004. Mesoscopic Modeling of Multicellular Tumor Spheroids: Validation through a Quantitative Comparison with Experimental Data. WSEAS Trans. Biol. Biomed. 1, 249.

Groebe, K., Mueller-Klieser, W., 1996. On the relation between size of necrosis and diameter of tumor spheroids. Int. J. Rad. Oncol. Biol. Phys. 34, 395.

Guiot, C., Degiorgis, P.G., Delsanto, P.P., Gabriele, P., Deisboeck, T.S., 2003. Does tumor growth follow a universal law. J. Theor. Biol. 225, 147.

Guiot, C., Delsanto, P.P., Carpinteri, A., Pugno, N., Mansury, Y., Deisboeck, T.S., 2006a. The dynamic evolution of the power exponent in a universal growth model of tumors. J. Theor. Biol. 240, 459.

Guiot, C., Pugno, N., Delsanto, P.P., 2006b. An elastomechanical model for tumor invasion. Appl. Phys. Lett. 89, 10.

Hamilton, G., 1998. Multicellular spheroids as an *in vitro* tumor model. Cancer Lett. 131, 29.

Helmlinger, G., Netti, P.A., Lichtenbed, H.C., Melder, R.J., Jain, R.K., 1997. Solid stress inhibits the growth of multicellular tumor spheroids. Nature Biotech. 15, 778.

Hufnagel, L., Teleman, A.A., Rouault, H., Cohen, S.M., Shraiman, B.I., 2007. On the mechanism of wing size determination in fly development. Proc. Natl Acad. Sci. USA 104, 3835.

Ingber, D.E., Prusty, D., Sun, Z., Betensky, H., Wang, N., 1995. Cell shape, cytoskeletal mechanics, and cell cycle control in angiogenesis. J. Biomech. 28, 1471.

Jiang, Y., Pjevisac-Grbovic, J., Cantrell, Ch., Freyer, J.P., 2005. A multiscale model for avascular tumor growth. Biophys. J. 89, 3884.

Kelm, J.M., Timmins, N.E., Brown, C.J., Fussenegger, M., Nielsen, L.K., 2003. Method for generation of homogeneous multicellular tumor spheroids applicable to a wide variety of cell types. Biotech. Bioeng. 83, 173.

Kleiber, M., 1932. Body size and metabolism. Hilgardia 6, 315.

Makarieva, A.M., Gorshkov, V.G., Li, B.-L., 2003. A note on metabolic rate dependence on body size in plants and animals. J. Theor. Biol. 221, 301.

Marusic, M., Bajzer, Z., Vuc-Pavlovic, S., Freyer, J.P., 1994. Tumor growth *in vivo* and as multicellular spheroids compared by mathematical models. Bull. Math. Biol. 56, 617.

McElwain, D.L.S., Pettet, G.J., 1993. Cell migration in multicell Spheroids: swimming against the tide. Bull. Math. Biol. 55 (3), 655.

Menchón, S.A., Condat, C.A., 2007. Macroscopic dynamics of cancer growth. Eur. Phys. J. Special Topics 143, 89–94.

Mueller-Klieser, W., 2000. Tumor biology and experimental therapeutics. Crit. Rev. Oncol./Hematol. 36, 123.

Murray, J.D., 2004. Mathematical Biology, vol. I, third ed. Springer, Berlin.

Nirmala, C., Rao, J.S., Ruifrok, A.C., Langfors, L.A., Obeyesekere, M., 2001. Growth characteristics of glioblastoma spheroids. Int. J. Oncol. 19, 1109.

Oudar, O., 2000. Spheroids: relation between tumour and endothelial cells. Crit. Rev. Onc./Hemat. 36, 99.

Perelson, A.S., Weisbuch, G., 1997. Immunology for physicists. Rev. Mod. Phys. 69, 1219.

Preziosi, L. (Ed.), 2003. Cancer Modelling and Simulation. Chapman and Hall/CRC, London, Boca Raton, FL.

Sansone, B.C., Delsanto, P.P., Magnano, M., Scalerandi, M., 2001. Effects of anatomical constraints on tumor growth. Phys. Rev. E 64, 021903.

Scalerandi, M., Sansone, B.C., 2002. Inhibition of vascularization in tumor growth. Phys. Rev. Lett. 89, 218101.

Scalerandi, M., Romano, A., Pescarmona, G.P., Delsanto, P.P., Condat, C.A., 1999. Nutrient competition as a determinant for cancer growth. Phys. Rev. E 59, 2206.

Scalerandi, M., Sansone, B.C., Condat, C.A., 2001. Diffusion with evolving sources and competing sinks: development of angiogenesis. Phys. Rev. E 65, 011902.

Scalerandi, M., Sansone, B.C., Benati, C., Condat, C.A., 2002. Competition effects in the dynamics of tumor cords. Phys. Rev. E 65, 051918.

Shraiman, B.I., 2005. Mechanical feedback as a possible regulator of tissue growth. Proc. Natl Acad. Sci. USA 102, 3318.

Thomson, K.E., Byrne, H.M., 1999. Modelling the internalization of labelled cells in tumour spheroids. Bull. Math. Biol. 61, 601.

Vernon, R.B., Angello, J.C., Iruela-Arispe, M.L., Lane, T.F., Sage, E.H., 1992. Reorganization of basement membrane matrices by cellular traction promotes the formation of cellular networks *in vitro*. Lab. Invest. 66, 536.

West, G.B., Brown, J.H., Enquist, B.J., 1999. The fourth dimension of life: Fractal geometry and allometric scaling of organisms. Science 284, 1677.

West, G.B., Brown, J.H., Enquist, B.J., 2001. A general model for otogenetic growth. Nature 413, 628.